JOURNAL OF GEOPHYSICAL RESEARCH VOLUME 65, No. 9 SEPTEMBER 1960

Direct Measurement of Particles Producing Visible Auroras

CARL E. MCILWAIN

Department of Physics and Astronomy
State University of Iowa
Iowa City, Iowa

Abstract. The nature of the particles producing two visible auroras at Fort Churchill, Canada, has been determined with the aid of rocket-borne detectors. Magnetic fields were used to separate the proton and electron components of the particle flux. It was found in each case that a major fraction of the auroral light was produced by electrons with energies of less than 10 kev.

IGY rocket II6.26F was fired into a quiescent auroral glow of about intensity I. The integral number energy spectrum of protons incident upon the atmosphere during this flight was measured to be approximately $2.5 \times 10^6 \exp(-E/30)$ protons/sec cm^2 ster over the range 80 to 250 kev, where E is the proton energy in kev. The observed altitude dependence of the electron energy flux could have been produced by an integral number energy spectrum equal to $2.5 \times 10^9 \exp(-E/5)$ electrons/sec cm^2 ster over the range 3 to 30 kev.

IGY rocket II6.27F was fired into a bright active auroral arc. At least 75 per cent of the light in this aurora was produced by nearly monoenergetic electrons with about 6-kev energy. The electron flux varied rapidly with time; peak values were about 5×10^{10} electrons/sec cm^2 ster. The presence of monoenergetic electrons strongly suggests an electrostatic acceleration mechanism.

INTRODUCTION

Extensive observations of auroras have been made with ground-based optical instruments [*Störmer*, 1955]. These investigations have provided excellent descriptions of most auroral phenomena. In particular, it has been established that the auroral light is due to energetic charged particles entering the earth's atmosphere (from the alignment of the auroral features with the magnetic field), and that some of the particles are protons (from the presence of Doppler-shifted H_α and H_β spectral lines). Other important results have been to determine the altitude distribution of the auroral light emissions; to establish the frequency of occurrence at different places on the earth; and to show the correlation with magnetic disturbances and events on the sun.

Rocket techniques greatly extend the kind of measurements that can be made. They should be capable of providing such information about the auroral particles as: (1) the relative number of electrons and protons; (2) the intensities of the particle fluxes; (3) the energy spectra of the particles; (4) the effects of the particles, such as the production of light and ionization. Information like this may eventually shed light on where the particles come from and how they are accelerated.

The present paper is based on the results obtained from two similar instrumentation packages that were placed on Nike-Cajun rockets and fired into visible auroras at Fort Churchill, Canada, during February 1958.

The first flight was into a faint aurora which contained the H_β line in its optical spectrum. An electron energy flux of about 20 ergs/sec cm^2 was measured by the rocket instruments. The proton detector in the rocket indicated the incidence of approximately 1 proton for every 1000 electrons. The second flight was into a bright auroral arc. The rocket-borne detectors suggest that the total energy flux was as high as 2000 ergs/sec cm^2 but the proton flux appeared to be less than on the previous flight.

PURPOSE

This exploratory investigation was intended to obtain a gross characterization of the particles that produce visible auroras. Accuracy and resolution were intentionally sacrificed in order to provide sensitivity to particles over a wide

range of intensities and energy. This choice was fortunate in view of the large time and spatial variations observed and the fact that many of the estimates of particle energies and intensities based on optical measurements were in error by more than an order of magnitude.

Apparatus

The rocket instrumentation contained three charged-particle detectors, a photometer, and a magnetometer (see Figs. 1 and 2).

Proton detector. The instrument designed to detect protons consists of a disk of CsI (Tl) scintillator 94 mg/cm^2 thick cemented to a photomultiplier tube (see Fig. 3). A 400-gauss magnetic field at the center aperture prevents electrons with less than 1-Mev energy from reaching the scintillator. The geometrical factor determined by the apertures is 3.5×10^{-3} cm^2 ster. About 40 micrograms/cm^2 of aluminum is evaporated on the crystal, reducing the light sensitivity by a factor of about 10^4. The aluminized crystal on the face of the RCA type 6199 photomultiplier tube is pictured in Figure 4. The detector is sensitive to all kinds of energetic ions, but for convenience it will be referred to as the 'proton detector.' In particular, the instrument is not capable of distinguishing α particles from protons.

The number of pulses from the photomultiplier tube corresponding to energy losses greater than 25 kev (45-kev protons before energy loss in the aluminum) are counted. In addition, the pulse height distribution corresponding to energy losses between 25 and 2500 kev is obtained by the following procedure:

1. In the rocket the pulse heights are converted into pulse lengths. The conversion process is inhibited for 10^{-2} second after the start of each conversion to prevent overlap and to permit input rates of up to 10^4/sec without distorting the distribution.

2. On the ground the pulse lengths are used to gate a stable oscillator, thus providing a digital representation of each pulse height.

3. The above procedure is identical in principle to the operation of the analog to digital converter in the 256-channel pulse height analyzer manufactured by Radiation Counter Laboratories. It is therefore possible to feed the signals derived from the rocket telemetry along with appropriate command signals into this analyzer to obtain the pulse height distribution at the detector output.

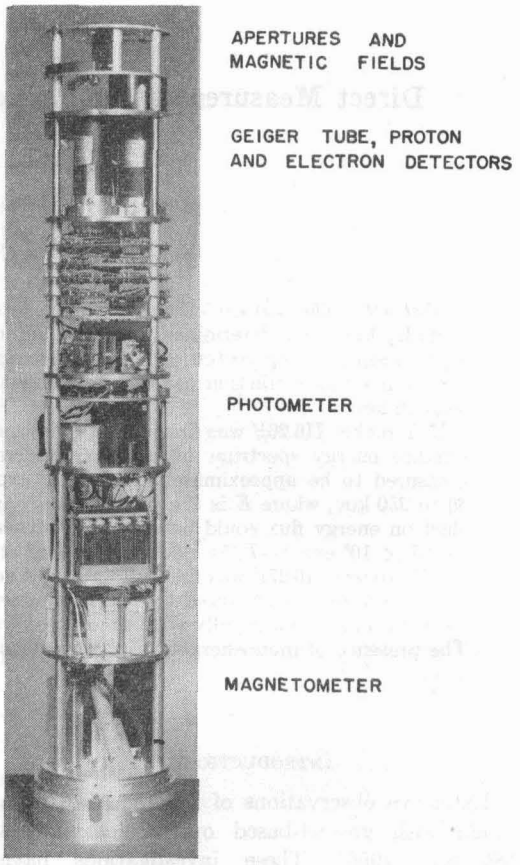

Fig. 1. Photograph of the rocket instrumentation, showing the placement of the detectors. The height of the instrumentation is 94 cm.

The pulse height distribution width, with this system using a pulse generator, is about 10 kev over the range of 25 to 500 kev. The energy resolution of the detector is approximately 30 per cent at 100-kev energy loss. The relative pulse height calibration of the instruments flown was determined using a pulse generator, and the absolute calibration was determined with Po^{210} α particles and Co^{57} γ rays.

Electron detector. Figure 3 shows a cross section of the electron detector. The magnetic field of the 250-turn coil focuses electrons from the ring-shaped aperture onto the ring of CsI (Tl) scintillator if the energy of the electrons

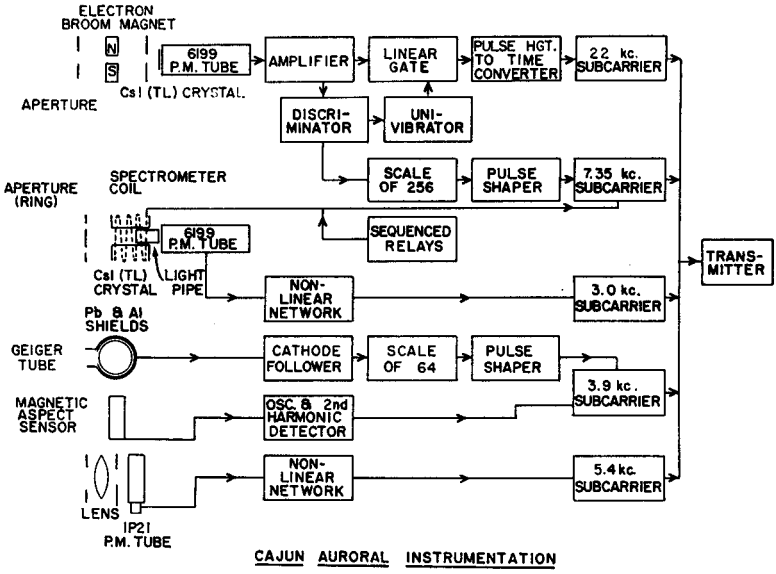

Fig. 2. Block diagram of the rocket instrumentation.

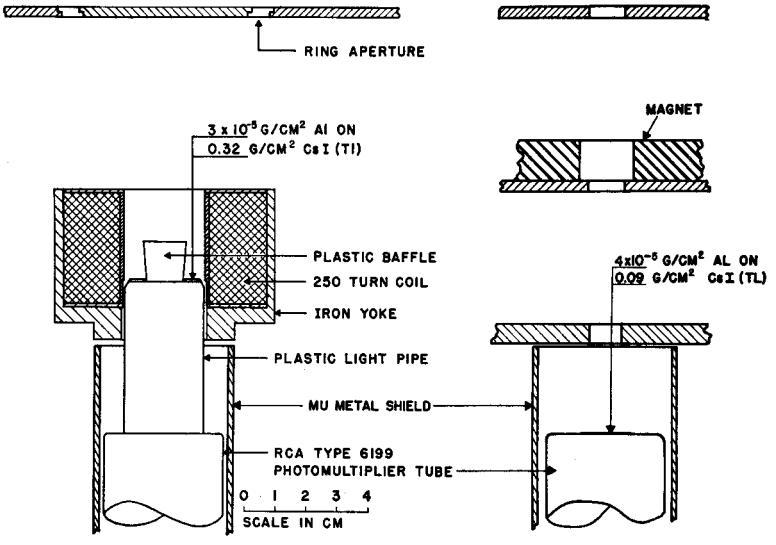

Fig. 3. Cross section of the electron (*left*) and proton (*right*) detectors, showing the geometry of the apertures and magnetic fields.

is within about a factor of 1.7 of an optimum energy set by the current in the coil. Since the photomultiplier tube pulses caused by very low energy electrons are too small to be counted individually, they are integrated, thus producing a current proportional to the average energy loss per second in the crystal. This current is passed through a nonlinear network which produces a voltage approximately proportional to the logarithm of the energy flux over the range 10^{-2} to 10^{2} ergs/sec cm^2 ster.

The crystal is covered by 30 μg/cm^2 of aluminum to reduce the light sensitivity. This aluminum film makes electrons with less than about 3-kev energy undetectable. The coil current is varied between 0 and 15 amperes by means of

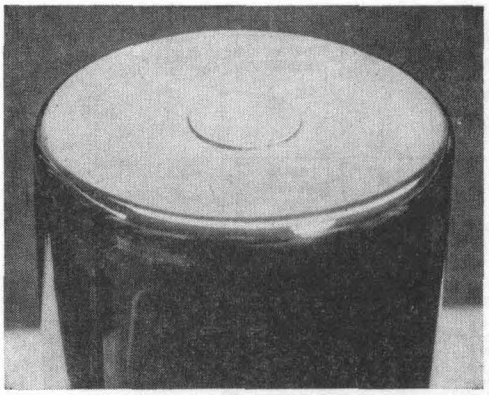

Fig. 4. A photograph of an aluminized disk of CsI crysal cemented to the face of a photomultiplier tube. The 1-cm-diameter crystal is the sensitive element in the proton detector.

sequenced relays in seven steps every 6 seconds. The highest current focuses electrons with energies up to 100 kev.

For this exploratory work, an intermediate baffle is omitted, therefore permitting rectilinear paths. This arrangement partially destroys the differential character of the instrument, but it has the advantage that the output with zero coil current is a measure of the total energy flux of all particles after passing through the 30 $\mu g/cm^2$ of aluminum covering the crystal. The geometrical factor for such rectilinear paths is 8.5×10^{-2} cm^2 ster. The geometrical factor for focused electrons is about twice this value.

The sensitivity of each crystal and photomultiplier tube combination was obtained by measuring the output as a function of the distance from a calibrated Po^{210} α-particle source. By performing this measurement before and after aluminization, the thickness of the aluminum was also determined. Unfortunately, an isotropic monoenergetic electron source cannot be easily obtained to provide an accurate calibration of the energy selectivity of the instrument. The energy best focused by the coil for different coil currents was obtained by rotating the instrument in two planes in a parallel monoenergetic electron beam.

Protons capable of penetrating the aluminum on the crystal are not appreciably deflected by the magnetic field; therefore, the changes in the detector output from the value at zero coil current can be due only to electrons.

Both the proton detector and the electron detector were aligned with the rocket axis. During the initial part of flight in the dense atmosphere an aerodynamic cone protected the detectors from damage. The cone was ejected 1 minute after launch. A Po^{210} α-particle source was placed on this cone to prove that it was ejected. A similar source was placed near the middle aperture of the proton detector. The pulse heights produced in the proton detector by these two sources provided a measure of the atmospheric density in the altitude range 10 to 25 km during ascent, and the source near the aperture provided a measure from 35 to 25 km during descent.

Geiger tube. Also included in the rocket instrumentation is a Victoreen type 1B85 Geiger counter, shielded by 1/16 inch of lead except for one side next to a 0.26 g/cm^2 aluminum window in the side of the instrumentation package. The geometrical factor for 1.0 to 5.0 Mev electrons in this configuration is 20 cm^2 ster. For lower energy electrons the detector has a low efficiency by way of X-ray production. The omnidirectional flux in electrons/sec cm^2 required to produce 1 count/sec in this manner was measured to be approximately 2×10^5 at 100 kev, 1.7×10^6 at 40 kev, 6×10^6 at 30 kev, 6×10^7 at 20 kev, and 10^{12} at 10 kev.

Rocket photometer. A photometer in the rocket instrumentation is used to measure the total directional intensity of visible auroral light. The photometer consists of an RCA 1P21 photomultiplier tube, apertures, a lens, and a Vycor window. The field of view is 3.5° by 5° directed perpendicular to the rocket axis. The photomultiplier tube current output is passed through a nonlinear network which provides a usable sensitivity over the range 10^{-3} to 4.0 ergs/sec cm^2 ster.

Ground photometer. A photometer with a 3.5° by 7° field of view directed near the vertical is used to help determine the best time to fire the rockets and to provide a measure of the auroral intensity during the rocket flights. Filters are not used with either the ground or rocket photometer. The photometers simply weight the auroral spectrum according to the S-11 photocathode spectral sensitivity curve. The absolute calibration of this photometer was obtained using a secondary standard low brightness source obtained from the Defence Research Northern Laboratory at Fort Churchill, Canada.

Aspect sensor. A flux gate magnetometer manufactured by the Schonstedt Engineering Company is used to determine the aspect of the rocket with respect to the magnetic field. The sensing element of the magnetometer is tilted 15° from the rocket axis to improve the accuracy of aspect determination when the rocket axis is close to alignment with the magnetic field. The magnetic field at Fort Churchill is inclined 6.3° from the vertical; therefore, for many purposes the angle measured by the magnetometer can be considered to be the angle to the vertical.

Altitude Determination

No radar or Doppler type of transponder was included in the instrumentation, in order to keep the total weight below 50 pounds. During the ascent, vents in the side of the outer instrumentation tube maintain the air density at the detectors near the ambient atmospheric density; therefore, the energy loss of the α particles from the Po^{210} sources placed above the proton detector provides a direct measure of the rocket altitude. During descent the absence of the aerodynamic cone causes the air density at the detectors to be much higher than the ambient atmospheric density. This 'ram' density is approximately equal to $1.29\ \rho\ (M^2 + 0.36)$, where ρ is the atmospheric density and M the Mach number [*Havens, Koll, and LaGow*, 1952].

An IBM 650 computer is used to obtain the complete rocket trajectory by starting with the measured time and altitude at second-stage burnout and trying different burnout velocities until an accurate fit to the measured ram density versus time during descent is obtained. The accuracy of this method is estimated to be better than ± 1 km. Stereoscopic photographs taken at the launch site and at a site 15 km to the west are used to determine the horizontal component of the rocket velocity at time of second-stage burnout. To determine the horizontal position of the rocket during the remainder of the flight, this velocity is assumed to be constant.

Performance

The instruments on both rocket flights performed as anticipated. The rocket antenna radiation pattern was nearly omnidirectional; therefore, no information was lost because of poor antenna orientation. The transmitter frequency on the second flight was somewhat unstable, however, and caused some loss of information.

The Nike-Cajun rocket has been used to carry payloads of similar weight to altitudes greater than 160 km. In these two rocket flights the peak altitudes were approximately 120 km. As the altitude and velocity at second-stage ignition were normal in both, the low performance was presumably due to low second-stage thrust.

The low peak altitudes achieved resulted in an appreciable degradation of the data, owing to the fact that the atmospheric pressure is not known well enough at these altitudes to correct for the air absorption accurately and to the impossibility of detecting the very-low-energy particles that are stopped or degraded in energy by the air remaining above the rocket.

Events during February 1958

A number of unusual geophysical events occurred during February 1958. A sudden commencement occurred at 0125 UT February 11 and was followed by a severe magnetic storm. A Forbush-type decrease [*Winckler, Peterson, Hoffman, and Arnoldy*, 1959; *Lockwood*, 1960] in the cosmic-ray intensity began at about 0200 UT February 11; by 066 UT sea-level neutron monitors registered 4 to 5 per cent decreases. On the night of February 11–12 a bright red aurora was observed to extend over a large range of latitudes and longitudes. The following two weeks were characterized by moderate magnetic activity and frequent occurrence of high-latitude auroras. The ground photometer records for the period February 10 through 25 were analyzed to obtain the percentage of time the auroral light intensity overhead at Fort Churchill was greater than various values. Excellent weather conditions permitted 80 hours of cloud-free observations to be obtained. Figure 5 shows that the night sky was never fainter than about 3×10^{-2} erg/sec cm^2 (column) during this period and that the occurrence of higher intensities decreased approximately as the inverse square of the intensity. It also shows that for only about 10 minutes during this 80-hour period was

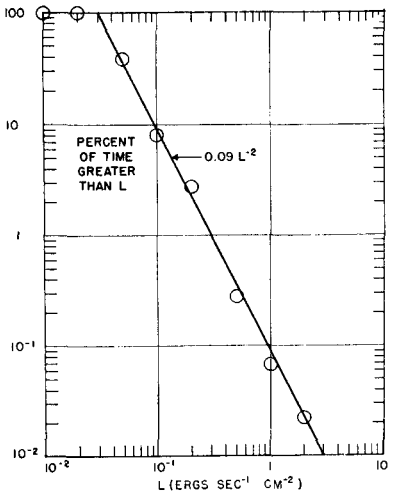

Fig. 5. Percentage of time the total visible overhead light flux (per cm² column) was greater than L during 80 hours of observation between February 10 and February 25, 1958, at Fort Churchill, Canada.

the auroral intensity greater than the maximum intensity that occurred during the flight of rocket II6.27F.

Results from IGY Rocket II6.26F

Characteristics of the aurora. IGY rocket II6.26F was fired at 05 hr 34 min 31 sec UT on February 22, 1958, into a faint quiescent auroral glow. As can be seen in Figure 6, which is a photograph taken by a high-speed all-sky camera at Fort Churchill when the rocket was at peak altitude, the auroral light intensity was fairly constant over a large area. The lower curve in Figure 7 shows the light intensity measured by the ground photometer during this flight. The average value is about 0.05 erg/sec cm² (col.) above the average night airglow value of 0.03 erg/sec cm² (col.). The night airglow intensity at lower latitudes is usually less than 0.01 erg/sec cm² (col.). The origin of this rather high night airglow intensity is unknown, but it may be the same as that of the light emissions that are labeled auroras because of their intensity and their time and spatial dependence. The absolute calibration of the ground photometer was roughly checked by visually noting that the 'night airglow' partly obscured the Milky Way. On account of the diffuse nature of the auroral light emission, the altitude of the lower boundary of the aurora during this rocket flight could not be measured from the ground.

Hydrogen spectrum. The most important ground observations made during this flight were the measurements by *Montalbetti* [1959] of the H_β spectral line intensity in the vertical direction at Fort Churchill (20 km from the rocket launching site). The spectrometer employed had a 7A resolution and scanned the region from 4580 to 4950 A in 12 seconds every 15 seconds. The average H_β intensity while the rocket was above 100 km was about 6×10^7 quanta/sec cm² (col.).

Protons. The flux of particles versus time recorded by the rocket proton detector is shown in Figure 8. The Geiger tube registered less than 0.2 particle/sec cm² ster with ranges greater than 1-Mev electrons in excess of the cosmic-ray flux; therefore the particles detected must have been protons, α particles, or heavier ions. It will be assumed that the particles were protons, since the H_α and H_β hydrogen spectral lines were recorded by the IGY patrol spectrograph at Fort Churchill whereas the helium line at 5876 A was not.

The integral energy spectrum, derived from the pulse height distribution while the rocket was between 120 and 122 km, is shown in Figure 9. The left-hand curve has been corrected for the energy losses in the layer of aluminum on the detector, and the right-hand curve has been corrected for the energy losses in the aluminum and the atmosphere remaining above the rocket. The integral proton energy spectrum incident upon the atmosphere is seen to be approximately fitted by the function $j\ (>E) = 2.5 \times 10^6 \exp(-E/30)$ protons/sec cm² ster over the range 80 to 250 kev, where E is the proton energy in kev. The proton energy spectrum obtained in this manner is not very dependent upon the model of the atmosphere used in extrapolating to above the atmosphere. The spectrum obtained from the proton flux versus altitude, however, is very strongly affected by the choice of the atmospheric model.

The atmospheric pressures at high altitudes given by various measurements and models differ by factors up to 4 or 5 to 1. Over the range 100 to 120 km, however, the ratios between these measurements and models are essentially

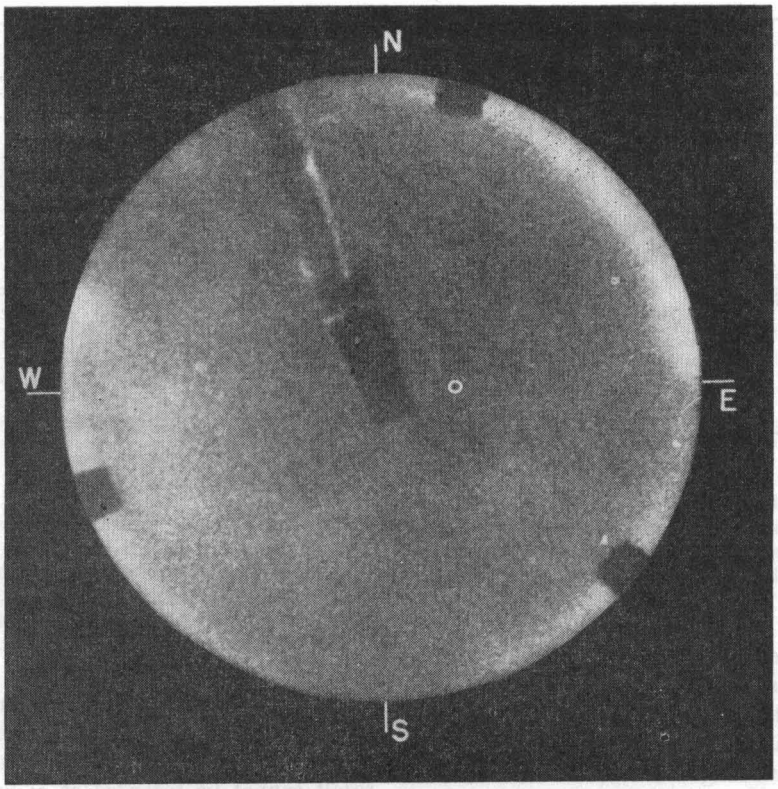

Fig. 6. All-sky photograph taken during the flight of rocket II6.26F.

constant. By assuming that the atmospheric pressure was a factor of 1.5 less than that of the *Rocket Panel* [1952] atmosphere, it was found that the proton energy spectrum obtained from the altitude dependence of the proton detector output is similar to the spectrum obtained from the pulse height distribution. This assumed atmospheric pressure is about a factor of 1.3 greater than the day-time pressure measured at Fort Churchill by *Horowitz, LaGow, and Guiliani* [1959]. For consistency, atmospheric pressures equal to those of the Rocket Panel model divided by 1.5 are used throughout this paper for pressures at altitudes above 95 km.

Figure 10 shows the proton spectrum derived from the pulse height distribution and from the altitude dependence during the rocket ascent and descent. The altitude and aspect curves shown in Figures 27 and 29 were used to obtain

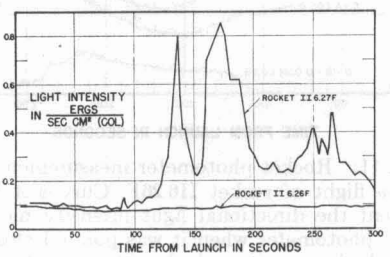

Fig. 7. Overhead light intensity measured by the ground-based photometer during the two rocket flights.

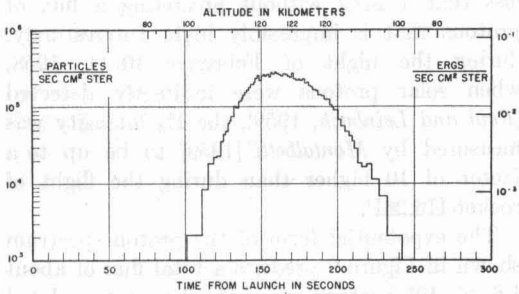

Fig. 8. Total flux of protons with energies greater than 45 kev measured by rocket II6.26F.

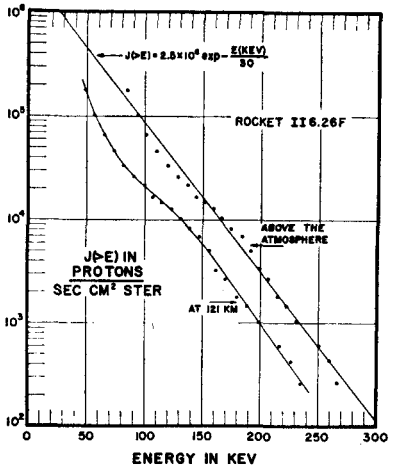

Fig. 9. Integral proton energy spectrum derived from the pulse height distribution obtained between 120 and 122 km by rocket II6.26F. The upper curve has been corrected for atmospheric absorption.

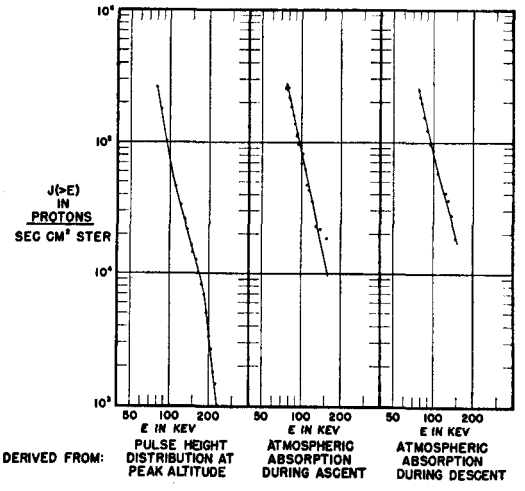

Fig. 10. Integral proton energy spectrum during the flight of rocket II6.26F. The points on the left-hand curve are the same as on the upper curve in Figure 9. The right-hand curves were derived from the number of protons with energies greater than 45 kev after atmospheric absorption.

the atmospheric absorption of the protons. It was also assumed that the directional intensity of protons above the atmosphere was constant in time and isotropic between 30° and 60° with respect to the magnetic field. It can be seen from the curves in Figure 10 that the proton integral energy spectrum between 80 and 200 kev can also be represented by $j\ (>E) = 2.5\ (E/1000)^{-4.5}$ protons/sec cm² ster, where E is in kev. This spectrum is similar in form to the one found for solar protons with energies between 30 and 300 Mev by *Anderson, Arnoldy, Hoffman, Peterson, and Winckler* [1959], but the constant for the auroral protons is lower by a factor of more than 10^7. It is obvious, however, that the power-law representation of the solar proton spectrum cannot be extrapolated to energies of less that 1 Mev without predicting a flux of protons that is impossibly high. Interestingly, during the night of February 10–11, 1958, when solar protons were indirectly detected [*Reid and Leinbach*, 1959], the H_β intensity was measured by *Montalbetti* [1959] to be up to a factor of 10 higher than during the flight of rocket II6.26F.

The expotential form of the proton spectrum shown in Figure 9 predicts a total flux of about 1.6×10^7 protons/sec cm² when extrapolated to zero energy with the assumption of isotropy over the upper hemisphere. This extrapolation would indicate that each proton produces about 4 H_β quanta, which is in fair agreement with the calculations made by *Chamberlain* [1954]. This result cannot be regarded as a direct measurement of the ratio of H_β quanta to incident protons since there is no reason for using this particular method for extrapolating to zero energy other than the fact that it gives a finite total proton flux.

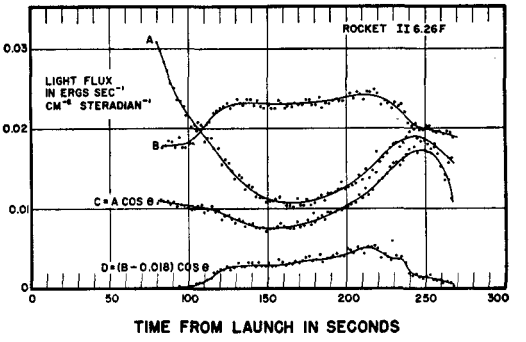

Fig. 11. Rocket photometer measurements during the flight of rocket II6.26F. Curves A and B represent the directional light intensity measured by the photometer when it was pointed closest to up and down, respectively. Curves C and D represent the measurements after corrections to give the light intensity from auroral emissions above and below the rocket.

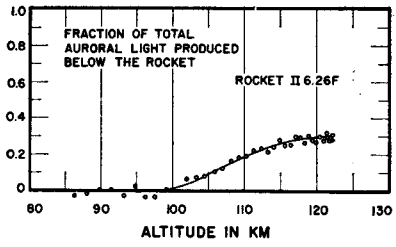

Fig. 12. Integral of the auroral luminosity versus altitude derived from curves C and D in Figure 11.

Rocket measurements of auroral light. The auroral light intensity measured by the rocket photometer during this flight is shown in Figure 11. Curves A and B are from measurements made when the photometer was directed closest to up and down, respectively, during each spin cycle. Curves C and D are from the same measurements, but they are corrected for the angle of the photometer to the vertical. The downward measurements were also corrected for a large background, presumably caused by auroral light reflected by the lower atmosphere and snow on the ground. The absolute intensity scale is uncertain by about a factor of 2, owing to the lack of a reference level for the logarithmic response curve. Figure 12 is a graph of $D/(D + C)$ from the measurements between 80 and 180 seconds shown in Figure 11 and therefore exhibits the fraction of auroral light produced below the rocket. This function is quite sensitive to the value taken for the background intensity. In particular, the slope in the vicinity of 120 km is subject to considerable error due to the low rocket velocity, which gave the background intensity more time to vary.

Electrons. The total energy flux versus time measured by the electron detector during this flight is shown in Figure 13. The dependence of the detector output upon the current in the focusing coil (see Fig. 23) indicates that most of this energy flux is due to electrons with energies of less than 40 kev.

The atmospheric absorption of the electron total energy flux can be used to obtain an estimate of the electron energy spectrum. If it is assumed that the light production efficiency of the atmosphere is constant between 100 and 120 km, the photometer measurements can also be used in finding the electron spectrum. It has been shown by *Young* [1956] and others that the average energy lost per electron by a beam of low-energy electrons in traversing an absorber is approximately equal to the energy E_0 of an electron with an end-point range equal to the

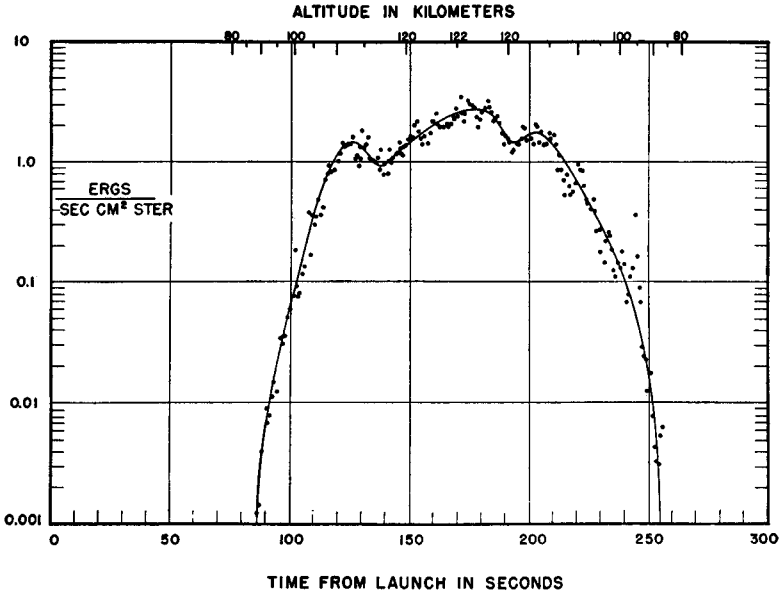

Fig. 13. Total energy flux versus time measured by the electron detector during the flight of rocket II6.26F after atmospheric and instrumental absorption.

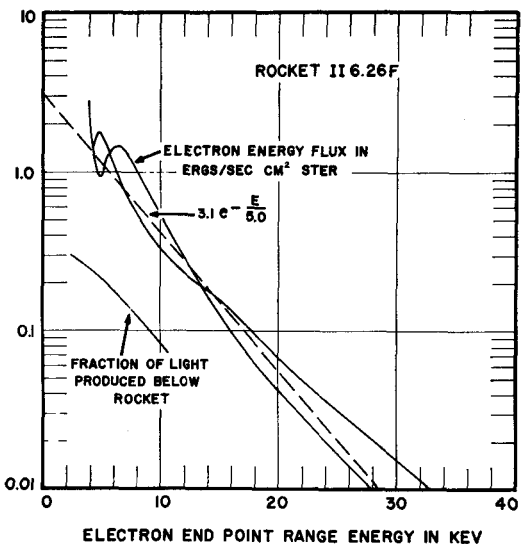

Fig. 14. The smooth curves in Figures 13 and 11 plotted against the electron energy which has a practical range equal to the atmospheric depth. The electron energy flux curve includes the additional absorption of the aluminum film covering the detector.

absorber thickness. In the present case of absorption by the high atmosphere in the presence of the relatively strong geomagnetic field, this approximation may not be good, but scattering probably controls the average electron trajectory more than the magnetic field does. If the integral number energy spectrum can be represented by a function of the form $c \exp(-E/b)$, where c and b are constants, the energy flux emerging from an absorber with an electron endpoint range energy of E_0 will be $cb \exp(-E_0/b)$. In Figure 14, the smooth curves of Figures 13 and 11 have been replotted against E_0.

The function 3.1 exp ($-E_0$/5.0 kev) ergs/sec cm² ster fits these curves within the uncertainty caused by time variations. The integral number energy spectrum incident upon the atmosphere is therefore approximately 2.5×10^9 exp ($-E$/5 kev) electrons/sec cm² ster over the range 3 to 30 kev. The exact electron energy spectrum may have been considerably different from the result of this rather crude analysis, but it must have had the same general characteristics. The curve derived from photometer readings in Figure 14 extrapolates to a value of 0.5 at zero energy rather than to a value of 1.0. This discrepancy indicates either that the electron spectrum given above explains only about one-half of the total energy flux or that the light production efficiency is higher in the very high atmosphere than in the 100- to 120-km region.

If it is assumed that the directional intensity of electrons was isotropic over the upper hemisphere, extrapolation of the above electron spectrum to zero energy indicates a total electron flux upon the atmosphere of about 1.6×10^{10} electrons/sec cm² and a total energy flux due to electrons of about 20 ergs/sec cm².

The efficiency of the atmosphere between 100 and 120 km for converting energy lost by auroral electrons into visible light energy is found to be about 0.2 per cent. This result is based on the spectral sensitivity and absolute calibration of the ground photometer, the relative light produced below 120 km measured by the rocket photometer, and the assumption that the electrons were isotropic over the upper hemisphere. The probable error of this result is about a factor of 2. It is regarded as unlikely that the efficiency quoted above is in error by more than a factor of 4.

Results from IGY Rocket II6.27F

Behavior of the aurora and magnetic field. IGY rocket number II6.27F was fired at 05 hr 48 min 32 sec UT on February 25, 1958, into a bright auroral arc. Figure 15 is a photograph taken during the first 30 seconds of the rocket flight from a site 15 km west of the rocket launcher. The short streak, just above the trace left by the expended first stage, was produced by the ignition and burning of the second-stage rocket.

This aurora began as a bright homogeneous arc about 330 km to the south at 0455 UT and extended without irregularities from horizon to horizon. At 0530 UT the aurora 'broke up,' the entire visible sky became brighter, and bright aurora rapidly progressed northward in an irregular fashion. At 0540 UT the bright northern edge of the aurora reached overhead at Fort Churchill. Coincident within ±3 minutes of the auroral 'break up' magnetometer traces at three stations changed from very quiet to very disturbed. At Fort Churchill, the Y and Z components of the magnetic field varied rapidly

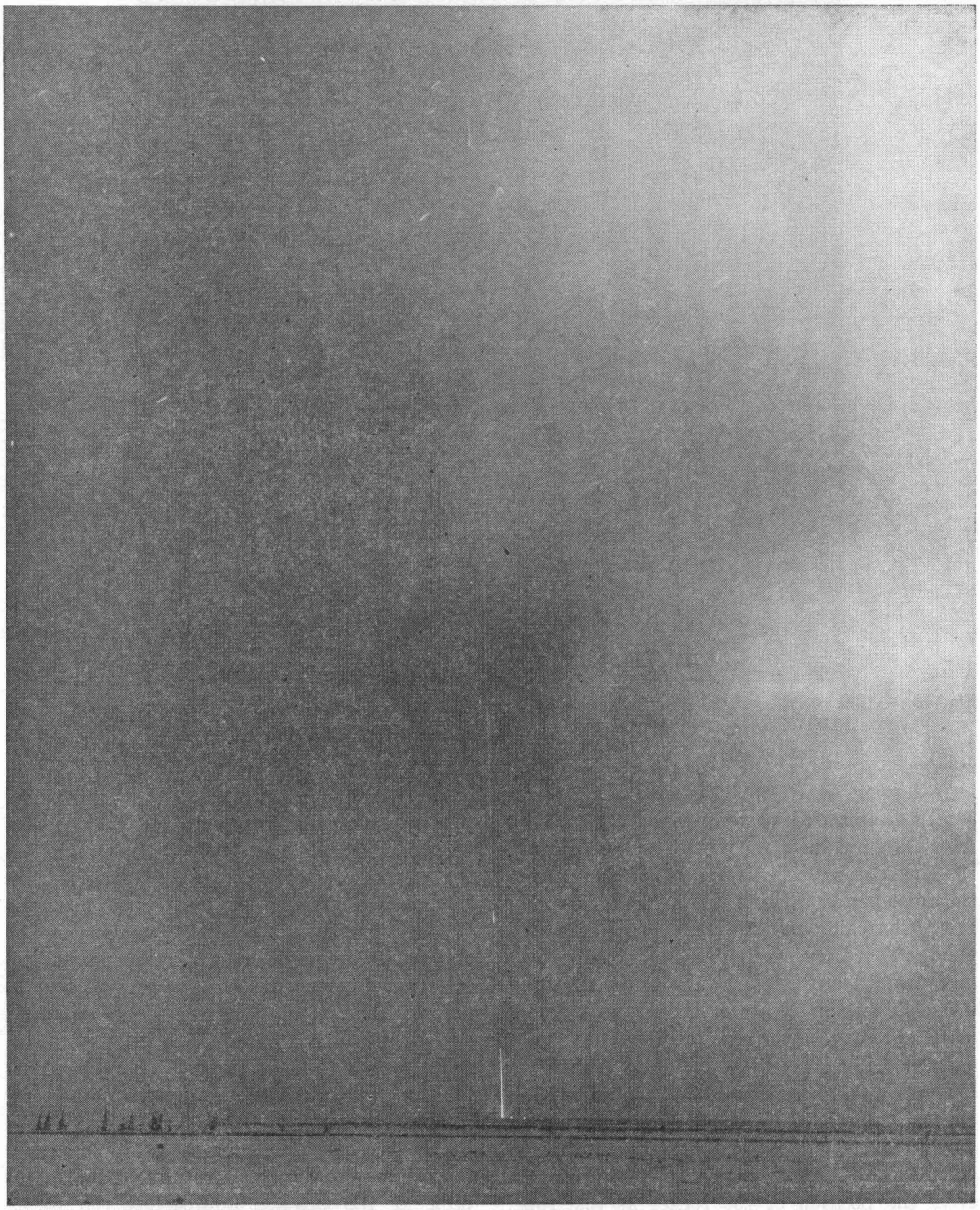

Fig. 15. Photograph taken during the first 30 seconds of rocket flight II6.27F from a site 15 km west of the rocket launcher. The traces produced during the burning periods of the first- and second-stage rockets are near the bottom and top of the photograph. The faint trace between these traces was produced by the expended first-stage rocket.

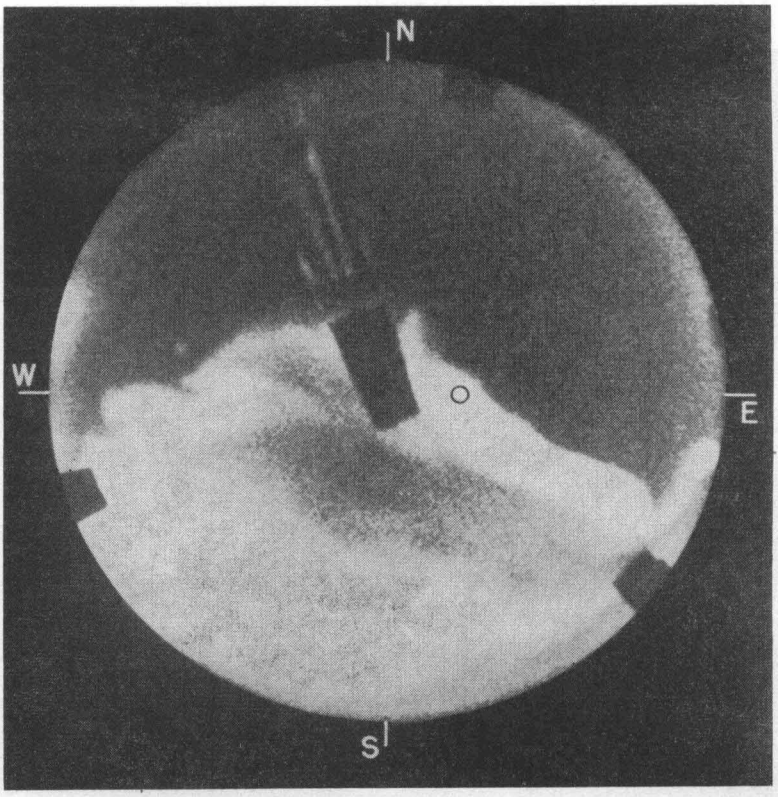

Fig. 16. All-sky-camera photographs taken at Fort Churchill 175 seconds after the launch of rocket II6.27F. The position of the rocket at this time is indicated by the small circle.

over a range of about 300 γ, and the X component disappeared, possibly off scale ($> 1000\ \gamma$). At O'Day, 130 km to the south of Fort Churchill, the single trace varied from 200 to 400 γ from the quiet-period value. At Bird, 250 km south of Fort Churchill, the X component decreased about 400 γ. Later the intense and rapidly varying auroral features filled most of the sky until 0700 UT, when the auroral brightness diminished. Fainter light emission persisted until dawn at 1100 UT.

Figure 16 is a photograph of this aurora taken at Fort Churchill 175 seconds after the launch of the rocket by a fast (f/0.71) camera directed down toward a hemispherical mirror. The circle gives the position of the rocket at this time. Figure 17 is a similar photograph taken at O'Day (140 km southwest of the rocket) 140 seconds after launch. Figure 18 is a photograph taken at Belcher (100 km southwest of the rocket) between 142 and 147 seconds after launch; it is one of many pairs of auroral-height-finding photographs made at Belcher and O'Day [*McEwen and Montalbetti,* 1958]. The position of the rocket is again indicated by a circle. The height scale refers to the northern edge of the aurora and shows the lower boundary to be about 110 km high. For other azimuths this scale must be modified to compensate for the different horizontal distances of the northern edge of the aurora.

The upper curve in Figure 7 shows the light intensity measured by the ground photometer during this flight. The light intensity measured by the rocket photometer shown in Figure 19 reveals that the auroral feature producing the peak at 135 seconds approached the rocket from the south but began to decrease in intensity just before reaching the rocket.

Absence of protons. In the number of pulses above the discrimination point in the proton detector, this flight was similar to flight II6.26F.

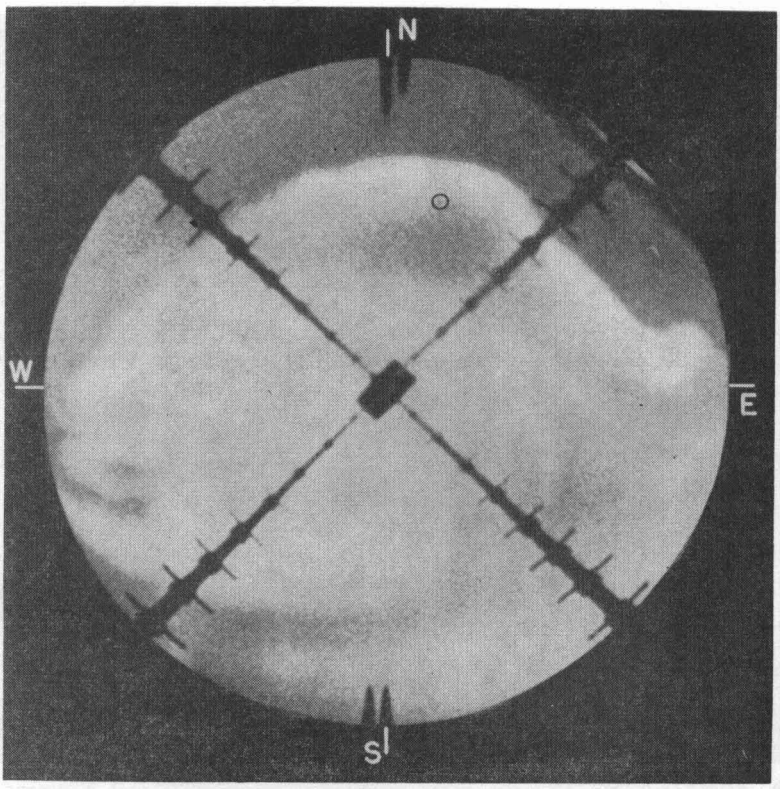

Fig. 17. All-sky-camera photograph taken at O'Day (140 km southwest of the rocket) 140 seconds after the launch of rocket II6.27F. The small circle indicates the position of the rocket.

Several factors combine, however, to indicate that in this flight most of these pulses were due to the light of the aurora. First, the quality of the layer of aluminum on the crystal was not as good as that on rocket II6.26F. Second, the discrimination point was lower, to the extent that a moderate number of photomultiplier tube noise pulses were counted even in total darkness. Third, the aurora was much brighter; and fourth, the flux of protons with greater than 100-kev energy was at least a factor of 10 less than during flight II6.26F. The pulse height distribution sharply decreased with increasing pulse height so that less than 1 out of every 50 pulses corresponded to energy losses in the crystal of greater than 50 kev. This indicates that less than 4×10^3 protons/sec cm^2 ster with energies greater than 100 kev were incident upon the atmosphere. No H_β spectral line could be detected during this flight.

Electrons. The electron detector on this flight measured total energy fluxes as high as 100 ergs/sec cm^2 ster. The energy flux versus time shown in Figure 20 in general follows the light intensity measured by the photometers but exhibits very rapid and irregular fluctuations. The output of the detector as a function of current in the focusing coil indicates that more than 90 per cent of this energy flux is due to electrons.

The energy spectrum of the electrons detected during this flight is very different from the electron energy spectrum measured on flight II6.26F. Instead of being distributed over a wide range of energies, the electrons in this case appear to have been nearly monoenergetic at about 6 kev. Since this energy is near the minimum energy detectable, the shape of the energy spectrum cannot be obtained with any precision. In the following paragraphs it will be shown, however, that less than 10 per cent of the total energy flux was due to electrons with greater

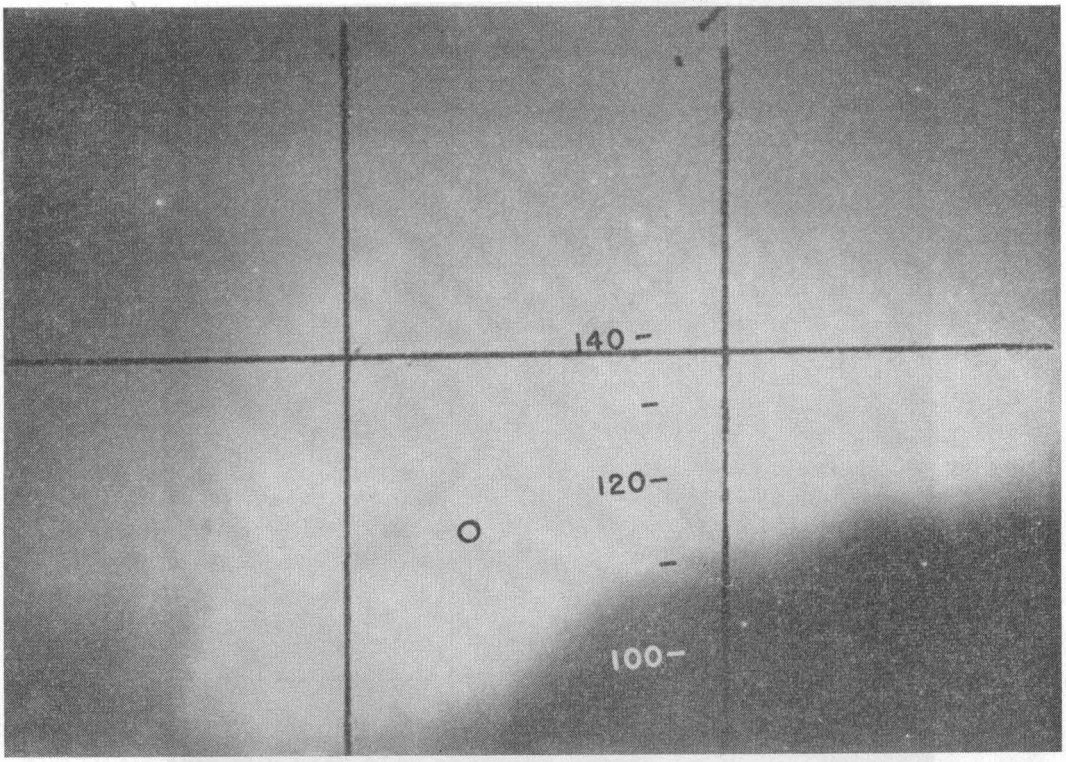

Fig. 18. Auroral height-finding photograph taken at Belcher between 142 and 147 seconds after the launch of rocket II6.27F. The altitude scale in kilometers refers to the northern edge of the aurora.

than 10-kev energy and that less than 25 per cent of the auroral light was produced by electrons with less than 3-kev energy.

Very-low-energy electrons. The low performance of the rocket and the absorption by the aluminum on the crystal make it impossible to estimate the flux of electrons with less than 4-kev energy by means of the electron detector. The rocket photometer measurements can, however, be used to obtain some information about these very-low-energy electrons. Figure 21, obtained similarly to Figure 12, shows the fraction of auroral light produced below the rocket as a function of altitude. The scatter of the measured values is due to the rapid time variations and possibly to changes in the electron spectrum. These measurements show that the auroral luminosity sharply decreased below 112 km, in good agreement with the results obtained by the auroral- height-finding photographs as illustrated in Figure 18. The curve in Figure 21 is the integral of the auroral luminosity versus altitude; it predicts that relatively little light was emitted at altitudes greater than 130 km. The apparent light emission at higher altitudes in Figure 18 is probably from auroral light produced closer to the camera.

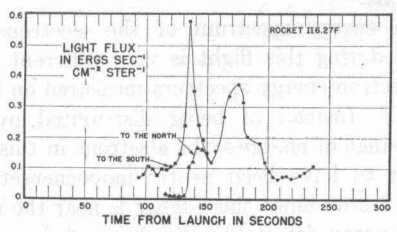

Fig. 19. Sum of the auroral light produced above and below rocket II6.27F measured by the rocket photometer. The light intensities looking slightly to the north and to the south were considerably different until 150 seconds after launch.

In the lower half of Figure 22 the data points shown in Figure 21 have been replotted with the altitudes converted to atmospheric depths. The resulting curve is too close to linear to have

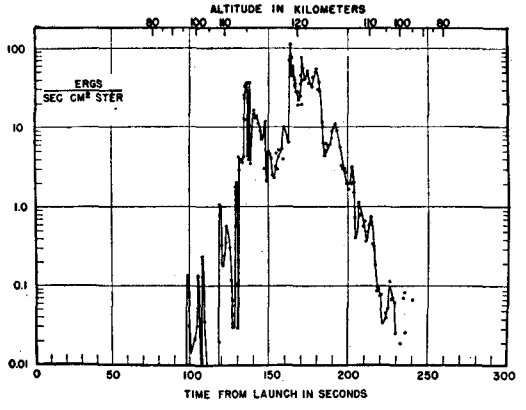

Fig. 20. Total energy flux versus time during the flight of rocket II6.27F.

been produced by electrons distributed in energy according to a simple power or exponential law but is very similar to the curve that might be expected from monoenergetic electrons. The initial energy of the electrons, corresponding to the range of 8×10^{-5} g/cm² given by this curve, could have been between 4 and 7 kev, depending on the electron angular distribution assumed and the model of the atmosphere used. Approximately 50 per cent of the auroral light was produced by these electrons in the last half of their range (40–80 μg/cm²). Therefore, these electrons probably produced at least 25 per cent of the auroral light in the first half of their range (0–40 μg/cm²), leaving less than 25 per cent of the auroral light to be produced by electrons with less than 3-kev energy.

Total electron flux. To obtain the dependence of the total energy flux upon atmospheric depth, the measurements shown in Figure 14 must be corrected for the large time variations.

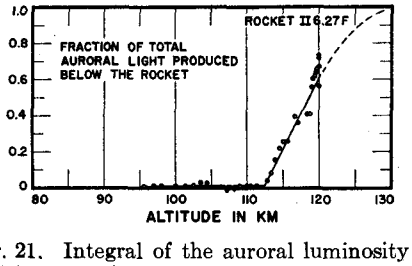

Fig. 21. Integral of the auroral luminosity versus altitude derived from the rocket photometer measurements between 160 and 240 seconds after the launch of rocket II6.27F.

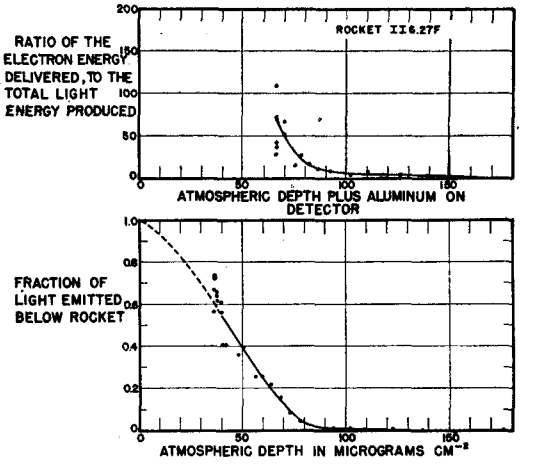

Fig. 22. The measurements shown in Figure 21 are plotted versus the atmospheric depth in the lower graph. The upper graph shows the ratio of the particle energy delivered to the crystal in the electron detector to the total visible light energy produced by the atmosphere as measured by the rocket photometer.

The rocket photometer measurements shown in Figure 19 give a crude indication of the time variations, and they were used to obtain the ratio of the electron energy delivered to the electron detector scintillator to the total light being produced along the line of force. These ratios, plotted against the total thickness of aluminum on the detector and atmosphere above, are shown in the upper half of Figure 22. Comparison with the lower half of the figure indicates that only about 20 per cent of the energy flux incident upon the atmosphere reached the scintillator when the rocket was at peak altitude. Assuming the directional intensity of electrons at the rocket to be constant over the upper hemisphere, the electron flux incident upon the atmosphere between 165 and 180 seconds after launch was approximately 2×10^{11} electrons/sec cm² if the energy per electron was 6 kev. This corresponds to a total energy flux of about 2000 ergs/sec cm². The possible error in assuming isotropy over the upper hemisphere is probably not serious, regardless of the initial angular distribution, because of atmospheric scattering and the fact that the detector averaged the flux from over a wide range of angles.

Absence of high-energy electrons. The rela-

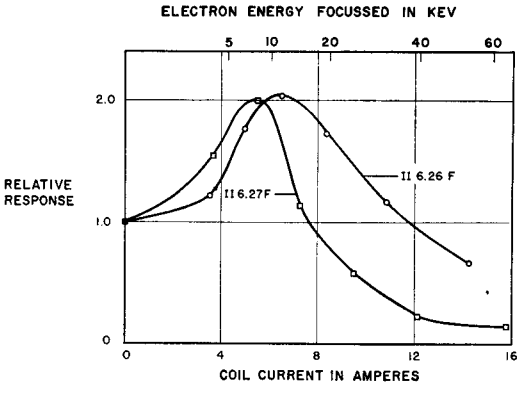

Fig. 23. Relative output of the electron detector as a function of current in the focusing coil during the two rocket flights.

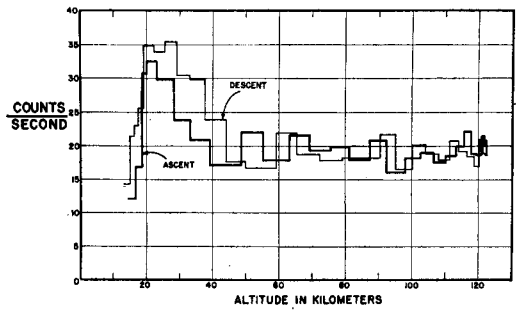

Fig. 24. Geiger tube counting rate versus altitude during rocket flight II6.26F.

tive absence of electrons with energies greater than 7 kev can be deduced from Figure 22, which shows that only about 1 per cent of the initial energy flux remained after absorption by 100 $\mu g/cm^2$ of material.

Comparison of the relative output of the electron detector versus coil current shown in Figure 23 with that of rocket II6.26F also shows the relative absence of higher-energy electrons. The points on these curves have an accuracy of only about ± 15 per cent, owing to the wide dynamic range covered by the analog output and to time variations during changes in coil current. The relative output of the detector versus coil current for isotropic monoenergetic electrons can be obtained in the laboratory by measuring the geometrical factor at different currents with a parallel pencil of monoenergetic electrons directed at the detector from different angles and positions. For practical reasons, the accuracy obtained to date with this procedure is rather poor, but the resulting function is very similar to the curve obtained during the flight of rocket II6.27F. Without an accurate knowledge of this function, the conversion of the curves in Figure 23 into electron energy spectra is impossible. A qualitative picture of the differential number energy spectra implied by these curves can be obtained by noting that the relative sensitivity of the detector for focused electrons increases approximately as the fourth power of the coil current. This can be seen from the following facts: The energy loss per electron in the scintillator increases as the first power of the electron energy; the differential range of magnetic rigidities focused is proportional to the coil current; the electron energy focused is approximately proportional to the square of the magnetic rigidity focused; and the magnetic rigidity focused is directly proportional to the coil current.

Further evidence for the relative absence of higher-energy electrons during this flight is the fact that the Geiger tube counted only cosmic rays. In the case of rocket II6.26F, the electron spectrum of $2.5 \times 10^9 \exp(-E/5)$ weighted by the measured efficiency of the detector predicts a contribution to the counting rate of about 3 counts/sec. Figure 24 shows the counting rate of the Geiger tube in rocket II6.26F versus altitude. The average rate above 50 km of 19.0 ± 0.3 counts/sec is to be compared with the average of 16.6 counts/sec obtained on four other rocket flights at Fort Churchill. The absence of a significant increase above 100 km, however, suggests that the difference of 2.4

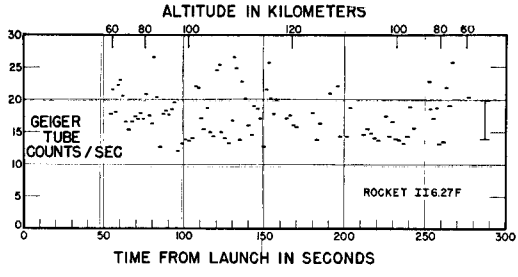

Fig. 25. Geiger tube counting rate versus time during the flight of rocket II6.27F. The vertical line to the right gives the probable error of the individual measurements.

counts/sec may have been caused by an increase in the cosmic-ray intensity.

Figure 25 shows the counting rate of the Geiger tube in rocket II6.27F versus time. The short bars represent the average counting rate for each 32 counts received, giving each bar a probable error of 3 counts/sec from the average value of 17.0 counts/sec. The lack of any statistically significant variation from the expected cosmic-ray counting rate implies that the intensity of 20- to 40-kev electrons during this flight was less than during the flight of rocket II6.26F even though the total energy flux was as much as 50 times greater.

Discussion

Electrons incident upon the atmosphere. Examination of the results presented in the preceding sections indicates that the luminosity of the two auroras investigated was primarily due to the incidence of energetic electrons upon the atmosphere. In each, the absolute intensity and altitude distribution of the auroral emissions could easily have been produced by the electrons detected by the rocket-borne instruments. Particle acceleration in the light-emitting regions, as by an atmospheric discharge, was therefore either absent or not important in the production of light.

Intensity of hydrogen spectrum. Chamberlain [1954] estimates that a 90-kev proton produces 50 H_α quanta in its total path length in the atmosphere, therefore converting about 10^{-3} of the proton energy into H_α quanta. The conversion efficiency would be higher for lower-energy protons. This efficiency is to be compared with the measured efficiency of 2×10^{-3} for the conversion of electron energy into all forms of visible light by the atmosphere between 100 and 120 km. It would appear that the H_α spectral line, in an aurora produced by protons only, should be almost as intense as the O I 5577 A line. Since the relative H_α intensity has never been reported to be this high, most auroral emissions in the 100-to 120-km region are probably due to electrons. *Omholt* [1959] also concludes, on the basis of the observed ratios of the H_β line intensity to the N_2^+ band intensity at 4709 A, that protons regularly supply only a minor part of the energy necessary to produce auroras.

Effective temperatures. The electron and proton energy spectra measured during the flight of rocket II6.26F can be represented within the accuracy of the measurements by Maxwell-Boltzmann energy distributions. The effective temperatures obtained are $(5.4 \pm 1) \times 10^7$ °K for the electrons and $(3.2 \pm 0.4) \times 10^8$ °K for the protons.

Many theories can be conjectured which give a qualitative explanation of these energy spectra [*Chamberlain,* 1958]. The choice between them must await further experimental results. Measurements of the energy spectra of the solar particles while in transit to the earth would be particularly valuable in this regard.

The electron energy spectrum measured during the flight of rocket II6.27F cannot be represented by a Maxwell-Boltzmann energy distribution. As was mentioned previously, the electron energy spectrum during this flight cannot be determined accurately from the available data. It was shown, however, that the spectrum decreased precipitously toward higher energies in the region of 10 kev but did not increase rapidly toward lower energies in the region below 4 kev. Quantitatively, this spectral form could be represented by a Maxwell-Boltzmann energy distribution with a temperature of about 6×10^7 °K except for the fact that far too few high-energy electrons were present. In common with the Maxwell-Boltzmann distribution, almost all particle energy spectra produced by acceleration mechanisms involving statistical processes predict a moderate number of particles with energies considerably higher than the average particle energy. Acceleration processes of a statistical nature therefore could not have been important in the history of the particles producing the aurora penetrated by rocket II6.27F. Acceleration processes involving electric fields might, however, produce an electron energy spectrum with a sharp high-energy cutoff.

Magnetic field instabilities. The rapid variations and distorted appearance of the aurora penetrated by rocket II6.27F are strong evidence for instabilities in the magnetic field somewhere along these lines of force.

The number of electrons incident upon the atmosphere during these flights was not sufficiently high to produce these instabilities. In

order to reach the atmosphere, however, auroral particles must be aligned to within $\pm 2°$ of the line of force in the vicinity of the magnetic equator. The particles producing auroral light are therefore probably only a small fraction of the total number of particles involved.

It is of interest to see whether the particles whose trajectories make angles greater than $\pm 2°$ to the line of force at the equator could have produced magnetic instabilities by assuming that their directional intensity was equal to the average directional intensity reaching the atmosphere. Whether the particle energy density is less or greater than the magnetic field energy density is often used as a criterion of whether the field is stable or unstable. For rocket II6.26F, this criterion would not be quite met even if the measured directional particle intensity is assumed to have extended over the full 4π steradians. For rocket II6.27F, however, an extension of the measured intensity over a solid angle of only about 0.3 steradian would have been sufficient to meet this criterion for instability. This result is consistent with the relative stability of the auroral features during the flight of rocket II6.26F and the indications of instability during the flight of rocket II6.27F.

Break-up of quiescent arcs. The particles with trajectories that do not reach the atmosphere are reflected back toward the equator by the converging magnetic field. If the injection mechanism did not also act as an efficient loss mechanism, the particles would be trapped and accumulate until the magnetic field could no longer contain them. The magnetic field would therefore become unstable. The ensuing rapid variations of the magnetic field would tend to perturb the trapped-particle trajectories into directions which result in the loss of particles by absorption in the atmosphere.

The build-up of trapped particles may correspond to the initial quiet arc phase of an auroral display and the subsequent break-up to the onset of magnetic instabilities. The rapid variations of the magnetic field would also tend to raise some of the particles to higher energies by Fermi-type accelerations. The particles detected by rocket II6.27F may have been freshly injected particles whose energy spectrum had been relatively unmodified by post-injection accelerations. The particles detected by rocket II6.26F may have been older particles whose energy spectrum had been extended toward higher energies while they were trapped in the magnetic field.

Comparison with results from IGY rocket NN3.03F. Concurrent with the rocket investigation of auroras reported in this paper, rocket auroral experiments were performed by Davis, Meredith, and Berg of the U. S. Naval Research Laboratory (now with the National Aeronautics and Space Administration). The results obtained by these investigators during the flight of rocket NN3.03F [*Meredith, Davis, Heppner, and Berg,* 1958; *Davis, Berg and Meredith,* 1960] are remarkably similar to those obtained during the flight of rocket II6.26F. In particular, the electron energy flux and the intensity of protons with energies greater than 70 kev were both within a factor of 3 of the corresponding measurements made during the flight of rocket II6.26F.

Auroral-zone X rays. The absence of high Geiger tube counting rates during these flights is in sharp contrast with the results obtained during previous auroral zone rocket flights [*Meredith, Gottlieb, and Van Allen,* 1955; *Van Allen,* 1957]. The high Geiger tube counting rates during the previous flights, however, can easily be explained by fluxes of electrons similar in number to those during the present flights if it is assumed that the effective temperature of the electrons was about a factor of 2 higher than during the flight of rocket II6.26F.

Comparison with trapped radiation. It has been suggested that auroral particles and particles trapped in the outer radiation zone are closely related [*Van Allen, McIlwain, and Ludwig,* 1959]. Since, to a certain extent, these two phenomena occupy the same region of space, some relationship is to be expected, but its nature remains obscure.

The total intensity of trapped electrons in the center of the outer zone [*Van Allen and Frank,* 1959; *Arnoldy, Hoffman, and Winckler,* 1960] is similar to the total flux of electrons producing visible auroras. The energy spectrum of the trapped electrons is a moderately strong function of time and spatial position. Many of the observations, however, can be explained by the spectral form $c \exp(-E/70 \text{ kev})$ measured at low altitudes near the inner edge of the outer

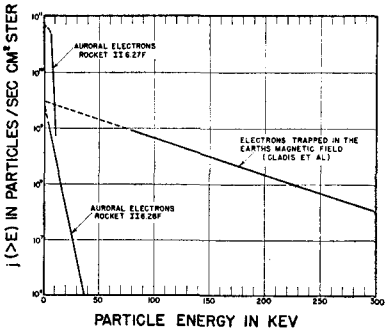

Fig. 26. Comparison of the integral electron energy spectra obtained by the two auroral rocket flights with the spectrum that may be present in the outer zone of trapped radiation.

zone by *Cladis, Chase, and Imhof* [1960; *Walt, Chase, Cladis, Imhof, and Knecht,* 1960]. It is interesting to note that the inner-zone electrons have a similar spectral form [*Holly and Johnson,* 1960]. These measurements of the trapped-electron energy spectrum can also be represented by a Maxwell-Boltzmann distribution, but with a temperature approximately an order of magnitude higher than the auroral electrons. The trapped-electron energy spectrum is compared with the auroral energy spectra in Figure 26. Some version of the processes suggested previously to explain the behavior of auroras may also be responsible for the trapped electrons, but many more detailed experiments must be performed in order to establish the origin of these particles.

Future Experiments

Auroral features take a great number of forms, many of which cannot be explained by simple modifications of the particle fluxes observed producing the auroras described in this paper. A properly instrumented earth satellite in a high-inclination orbit would be invaluable in determining the nature of the particles producing the different auroral features.

The detectors in future rockets and satellites should be capable of measuring the absolute energy spectra and angular distribution of electrons and protons over the energy range of at least 1 kev to 1 Mev. Simultaneous measurements with such instruments of the particles in transit from the sun, of the particles in the regions where the auroral particles are injected (and/or accelerated), and of the particles producing a visible aurora should be capable of revealing the true nature of this bewildering phenomenon.

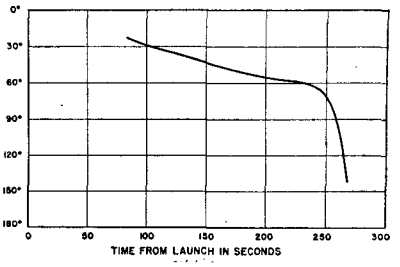

Fig. 27. The angle between the particle detectors and the negative of the magnetic field vector during the flight of rocket II6.26F.

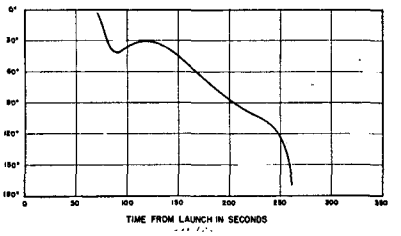

Fig. 28. The angle between the particle detectors and the negative of the magnetic field vector during the flight of rocket II6.27F.

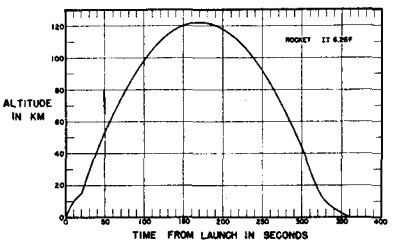

Fig. 29. Altitude of rocket II6.26F versus time.

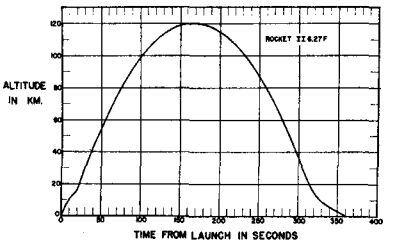

Fig. 30. Altitude of rocket II6.27F versus time.

Conclusion

The light emitted by the atmosphere below 120 km during two different auroras was found to be produced by low-energy electrons. Protons were detected in one, but the intensity was too low to contribute appreciably to the light emitted below 120 km.

The electron and proton energy spectra derived from measurements made during the flight of rocket II6.26F can be represented by Maxwell-Boltzmann distributions with temperatures of 5.4×10^7 and 3.2×10^8 degrees Kelvin, respectively. The energy spectrum of the electrons producing the aurora penetrated by rocket II6.27F, however, did not have a high-energy tail. The acceleration mechanism producing these nearly monoenergetic electrons therefore presumably did not involve a statistical type process.

During both rocket flights there was a striking absence of electrons with greater than 50-kev energy. The fact that the rocket-borne Geiger tube counting rates were less than a factor of 1.2 above the expected cosmic-ray rate is in great contrast to the very high counting rates anticipated on the basis of previous auroral-zone rocket flights. The total electron flux in these auroras was similar to the electron flux in the outer zone of trapped radiation, but the individual electron energies of the trapped electrons are typically an order of magnitude higher.

Acknowledgments. I wish to thank Professor James A. Van Allen for making this investigation possible and for his suggestions and guidance in the construction of the instruments and the analysis of the results.

The assistance of Mr. D. C. Enemark in the design and preparation of the many electronic circuits is gratefully acknowledged.

Many important optical observations of the auroral features were made by the Defence Research Northern Laboratory of the Canadian Department of National Defence. In particular I wish to thank Dr. R. Montalbetti, Mr. D. McEwen, and Mr. H. Lutz for obtaining the H_β spectral intensity and many photographs of the auroras penetrated by the rockets.

I wish to express appreciation to the many U. S. Army and Navy personnel who assisted in the rocket-launching operations.

I am grateful to Mr. H. Hills and Mrs. A. Hudmon for the reduction and analysis of the telemetry records.

The investigation was supported by the National Academy of Sciences and the National Science Foundation through their US/IGY Project 10.1 and by the joint program of the Office of Naval Research and the Atomic Energy Commission.

References

Anderson, K. A., R. Arnoldy, R. Hoffman, L. Peterson, and J. R. Winckler, Observations of low-energy solar cosmic rays from the flare of 22 August 1958, *J. Geophys. Research, 64,* 1133–1147, 1959.

Arnoldy, R. L., R. A. Hoffman, and J. R. Winckler, Observation of the Van Allen regions during August and September 1959, I, *J. Geophys. Research, 65,* 1361–1376, 1960.

Chamberlain, J. W., The excitation of hydrogen in aurorae, *Astrophys. J., 120* 360–366, 1954.

Chamberlain, J. W., Theories of the aurora, *Advances in Geophys., 4,* 109–215, Academic Press, New York, 1958.

Cladis, J. B., L. F. Chase, and W. L. Imhof, Energy spectra and spatial distributions of electrons trapped in the earth's magnetic field, *Bull. Am. Phys. Soc.,* [2] *5*(1), 46, 1960.

Davis, L. R., O. E. Berg, and L. H. Meredith, Direct measurements of particle fluxes in and near auroras, *Proc. Cospar Space Sci. Symposium,* North Holland Publishing Co., Amsterdam, 1960.

Havens, R. J., R. T. Koll, and H. E. LaGow, The pressure, density, and temperature of the earth's atmosphere to 160 kilometers, *J. Geophys. Research, 57,* 67, 1952.

Holly, F. E., and R. G. Johnson, Measurement of radiation in the lower Van Allen belt, *J. Geophys. Research, 65,* 771–772, 1960.

Horowitz, H. E. LaGow, and J. Guiliani, Fall-day auroral-zone atmospheric structure measurements from 100 to 188 km, *J. Geophys. Research, 64,* 2287, 1959.

Lockwood, J. A., Decrease of cosmic-ray intensity on February 11, 1958, *J. Geophys. Research, 65,* 27–37, 1960.

McEwen, D. J., and R. Montalbetti, Parallactic measurements on aurorae over Churchill, Canada, *Can. J. Phys., 36,* 1593–1600, 1958.

Meredith, L. H., L. R. Davis, J. P. Heppner, and O. E. Berg, Rocket auroral investigations, *IGY Rocket Rept. Ser. 1,* 169–178, National Academy of Sciences, National Research Council, Washington, D. C., 1958.

Meredith, L. H., M. B. Gottlieb, annd J. A. Van Allen, Direct detection of soft radiation above 50 kilometers in the auroral zone, *Phys. Rev., 97,* 201–205, 1955.

Montalbetti, R., Photoelectric measurements of hydrogen emissions in aurorae and airglow, *J. Atmospheric and Terrest. Phys., 14,* 200, 1959.

Ohmholt, A., Studies on the excitation of aurora borealis, 1, The hydrogen lines, *Geofys. Publikasjoner, 20*(11), 1–40, 1959.

Reid, G. C., and H. Leinbach, Low-energy cosmic-ray events associated with solar flares, *J. Geophys. Research, 64,* 1801–1805, 1959.

Rocket Panel, Pressures, densities, and temperatures in the upper atmosphere, *Phys. Rev.*, *88*(5), 1027–1032, 1952.

Störmer, C., *The Polar Aurora,* Oxford University Press, London, 1955.

Van Allen, J. A., Direct detection of auroral radiation with rocket equipment, *Proc. Natl. Acad. Sci. U. S. 43,* 57–92, 1957.

Van Allen, J. A., and L. A. Frank, Radiation measurements to 658,300 kilometers with Pioneer IV, *Nature, 84,* 219–224, 1959.

Van Allen, J. A., C. E. McIlwain, and G. H. Ludwig, Radiation observations with satellite 1958ε, *J. Geophys. Research, 64,* 271–286, 1959.

Walt, M., L. F. Chase, J., J. B. Cladis, W. L. Imhof, and D. J. Knecht, Energy spectra and spatial distributions of electrons trapped in the earth's magnetic field, *Proc. Cospar Space Sci. Symposium,* North Holland Publishing Co., Amsterdam, 1960.

Winckler, J. R., L. Peterson, R. Hoffman, and R. Arnoldy, Auroral X-rays, cosmic rays, and related phenomena during the storm of February 10–11, 1958, *J. Geophys. Research, 64,* 597–610, 1959.

Young, J. R., Penetration of electrons and ions in aluminum, *J. Appl. Phys., 27,* 1–4, 1956.

(Manuscript received June 10, 1960.)